The high-temperature structure of lead magnoniobate

1994 J. Phys.: Condens. Matter 6 4021

(http://iopscience.iop.org/0953-8984/6/22/001)

J. Phys.: Condens. Matter 6 (1994) 4021–4027. Printed in the UK

The high-temperature structure of lead magnoniobate

S Vakhrushev†, S Zhukov‡, G Fetisov‡ and V Chernyshov‡

† A F Ioffe Physico-Technical Institute, 26 Politekhnicheskaya, St Petersburg 194 021, Russia

‡ Department of Chemistry, Moscow State University, Moscow 119 899, Russia

Received 2 August 1993

Abstract. The results of x-ray diffraction measurements of a lead magnoniobate single crystal—$PbMg_{1/3}Nb_{2/3}O_3$, performed on a four-circle diffractometer with Mo Kα radiation, are described. It is confirmed that even at relatively high temperatures lead ions are shifted from the high-symmetry position. It is shown that these shifts are random both in length and direction. A spherical layer model is proposed for the adequate description of the experimental data. The correspondence between the crystal structure and the physical properties of the crystal is discussed.

1. Introduction

It is well known that the disordered perovskite-like crystals with non-isovalent ions in equivalent positions reveal a number of unusual physical properties at both low and high temperatures [1,2]. The lead magnoniobate crystal $PbMg_{1/3}Nb_{2/3}O_3$ (PMN) could be considered as a model object for such compounds. In spite of the large number of papers devoted to the investigation of PMN and its analogues, the microscopic nature of the observed anomalies is not clear yet. The properties of PMN at low temperatures such as the appearance of the broad temperature-dependent maximum in the frequency dependence of the dielectric permittivity $\varepsilon(T)$ [3], nearly logarithmic dispersion of the ε below this maximum and acoustic anomalies [4] could be explained by the phase transition to the correlated dipole glass state [5]. This conclusion is in good agreement with the results of x-ray and neutron scattering measurements, that do not show any distortion of the cubic lattice at temperatures down to 8 K [6]. At the same time, the investigations of PMN at high temperatures have revealed [3,7,8] that in this region also its properties are not identical to those of the usual perovskite-like ferroelectrics. It is necessary to mention the results of [7], where a strong first-order Raman scattering, forbidden in centrosymmetric crystals, was found in PMN at high temperatures. In [7] it was also shown that this scattering could not be explained by the break of the translational symmetry due to the random distribution of the Mg^{2+} and Nb^{5+} ions, but implies a distortion of the ideal perovskite lattice. It is absolutely clear that for the adequate interpretation of the observed physical properties the precise determination of the PMN structure both at low and high temperatures should be done. The existing papers concerned with the refinement of the PMN structure [6,9,10] concern ceramic samples and a very limited number of peaks was used for the refinement.

2. Experimental details

Here we report the results of an x-ray diffraction study of PMN structure over the temperature range 100–573 K. Investigated crystals were grown by spontaneous crystallization from

the solution in the melt of PbO [11]. Spherical samples 0.3 mm in diameter were prepared from the grown crystals. X-ray diffraction experiments were carried out on the CAD-4 Enraf-Nonius diffractometer (Mo Kα radiation, $\lambda = 0.71145$ Å^{-1}, graphite monochromator). Integrated intensities of reflections were measured by ω-scan with a scanning speed of 27° min^{-1} and a scan interval of $1.5+0.8\tan(\theta)$. The measurements at low and high temperatures were performed with an Enraf-Nonius Universal Low Temperature Device FR524 and an FR559 High Temperature Attachment to the CAD-4 with automatic temperature control. Cooling of the sample on the diffractometer was achieved by a gas stream of cold nitrogen and heating by a hot air stream. Temperature stability provided during x-ray experiments was not worse than 1 K. A special thermostable glue was used to fix the sample on the quartz holder.

Four x-ray diffractograms were obtained at 110 K, 224 K, 293 K and 573 K. The reflection integrated intensities were measured over a quarter of the reflection sphere up to $\sin(\theta)/\lambda \leqslant 0.8$ Å^{-1} at 573 K and over half of the sphere up to $\sin(\theta)/\lambda \leqslant 0.95$ Å^{-1} for the other cases. 457 reflections with $I > 3\sigma(I)$ were collected at 573 K and 1152 reflections in each experiment at the other temperatures. After averaging the equivalent reflections ($3.5\% \leqslant R \leqslant 4.2\%$) this gave 57 and 75 independent reflections, correspondingly, that were used for crystal structure solution with the aid of SDP-AE1 computer programs [12, 13].

3. Results

3.1. General description

Let us first consider the experimental data in detail. (i) It was shown by neutron scattering experiments [5, 14, 15] that the strongly temperature-dependent diffuse scattering (DS) is observed in the vicinity of the reflections with odd sums $(h + k + l)$ of Miller indexes. In the present experiments we have found that the integrated intensity of DS is negligible in comparison with that of the Bragg reflections at 573 K but drastically increases with cooling and surpasses the latter at 110 K in the vicinity of some reciprocal lattice points. So strong DS was a great obstacle for precise structure analysis at 110 K and 224 K which would be possible only with the detailed investigation of the intensity profiles of all measured reflections that we are planning to perform in the future. But it is possible to neglect the DS contribution at 573 K and 293 K and solve the crystal structure properly. (ii) Some conclusions about the static distortions in the crystal structure could be drawn from the analysis of the dependence of the Bragg reflection intensities upon the value of $\sin(\theta)/\lambda$ which is proportional to the length of scattering vector $|k|$. The experimental data obtained at 573 K and 293 K corrected for absorption are shown in figures 1 and 2. It should be mentioned that for an ideal perovskite structure ABO_3 four families of reflections could be chosen having the structure factors $F(k)$ of the form

$$(2h+1\ 2k+1\ 2l+1)F(k) = f_A \exp(-M_A) - f_B \exp(-M_B) + 3f_O \exp(-M_O) \quad (1)$$

$$(2h+1\ 2k\ 2l)F(k) = f_A \exp(-M_A) - f_B \exp(-M_B) - f_O \exp(-M_O) \quad (2)$$

$$(2h+1\ 2k+1\ 2l)F(k) = f_A \exp(-M_A) + f_B \exp(-M_B) - f_O \exp(-M_O) \quad (3)$$

$$(2h\ 2k\ 2l\ )F(k) = f_A \exp(-M_A) + f_B \exp(-M_B) + 3f_O \exp(-M_O) \quad (4)$$

where f_A, M_A, f_B, M_B and f_O, M_O are atomic scattering factors and Debye–Waller factors for A, B and O ions. Debye–Waller factors in the harmonic approximation could be presented as

$$M_x = (k \cdot \langle u_x \rangle)^2$$

where u_x are the thermal displacements of ion x. This means that the dependence of the partial contribution of ion x to the structure factor on scattering vector length $|k|$ has Gaussian shape. From (1)–(4) one can easily see that for undistorted perovskite crystals the dependences of the Bragg peak intensities on the $\sin(\theta)/\lambda$ value should follow four curves monotonically decreasing as $\sin(\theta)/\lambda$ increases. Moreover, neglecting the scattering on the oxygen ions, it is clear that the curves for families 1 and 2 should always be below those for families 3 and 4.

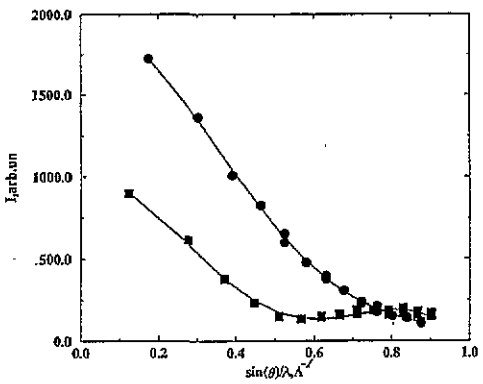

Figure 1. The dependence of the integrated intensity of the Bragg peaks on $\sin(\theta)/\lambda$ at 573 K. Squares correspond to the $(2h+1\ 2k+1\ 2l+1)$ reflections—family 1; circles correspond to the $(2h\ 2k\ 2l)$ reflections—family 4.

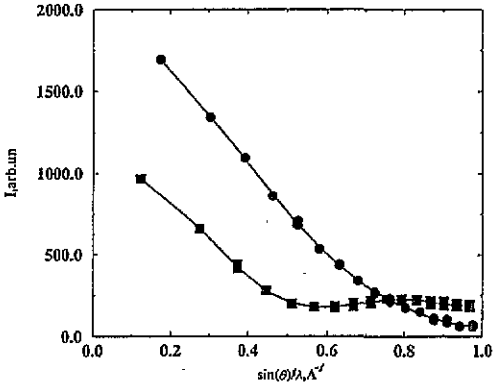

Figure 2. The dependence of the integrated intensity of the Bragg peaks on $\sin(\theta)/\lambda$ at 293 K. Squares correspond to the $(2h+1\ 2k+1\ 2l+1)$ reflections—family 1; circles correspond to the $(2h\ 2k\ 2l)$ reflections—family 4.

At the same time, from figures 1 and 2 one can easily see that for $\sin(\theta)/\lambda > 0.6$ Å^{-1} the experimental curves behave in a different way: the curve for family 2 displays a minimum at $\sin(\theta)/\lambda = 0.7$ Å^{-1} and crosses the curve for family 3 at $\sin(\theta)/\lambda = 0.8$ Å^{-1}. Such behaviour could be explained by the existence of the static displacements of the ions in addition to the usual thermal displacements. It has been shown [16, 17] that such static displacements could lead to the appearance of strong non-monotonic dependence of the scattering intensity on k. In the simplest case of uncorrelated shifts one should write in (1)–(4) $\exp(-M_x^1)\cos(k \cdot \Delta_x)$ instead of $\exp(-M_x)$, where M_x^1 describes the decreasing of the structure factor due to the thermal vibration and the Δ_x is an average static shift of ion x. In such a case after substitution the isotropic structure factor described by (1)–(4) becomes anisotropic, depending on the direction of k as well as its length [16]. On the other hand it can be seen in figures 1 and 2 that all data points follow smooth curves and do not depend on the direction of the scattering vector. This leads us to the conclusion that there is no specific direction of the ionic shifts in the crystal.

3.2. Spherical layer model

Now we consider how such an isotropic situation could be described. Let us suppose that x atoms are not situated in specific positions, but are shifted distance Δ_x in a random direction. In such a case, after averaging over the crystal volume one would obtain an average cell in which an x atom would be distributed over the surface of the sphere with radius Δ_x. Making an assumption that the scattering in the crystal with atoms shifted in random directions is

equivalent to the scattering in the crystal constructed from such averaged cells, one can obtain a simple expression for the structural factors and the value of Δ_x could be easily obtained in the process of structure refinement. The structural factor for the averaged crystal could be written in the following way:

$$F_x(k) = \lim_{N\to\infty}\left[(1/N)\sum_{n=1}^{N} f_x(k)\,\exp(-M_x)\,\exp(2\pi i \boldsymbol{k}\cdot\boldsymbol{r}_n)\right]$$

where $\boldsymbol{r}$ are the radius vectors of N points uniformly distributed over the spherical surface. The $1/N$ factor is introduced for normalization purposes. After all necessary transformation $F(k)$ could be written as

$$F_x(k) = f_x(k)\,\exp(-M_x)\frac{\sin(2\pi k\Delta_x)}{2\pi k\Delta_x}.$$

All necessary corrections for such a model were made in the AE1 [13] program used for the structure refinement.

3.3. Structure refinement

For the description of the experimental data we have used seven different models. We did not take into account the results of TEM measurements [20, 21], where nanometre regions of the non-stoichiometric $PbMg_{1/2}Nb_{1/2}O_3$ were observed. In our foregoing paper on the structure refinement of partly ordered $PbSc_{1/2}Ta_{1/2}O_3$ it was shown that this ordering does not affect results related to the observation of random Pb shifts. The obtained results are presented in table 1. In all cases instead of f-atomic curves for the Mg and Nb atoms an averaged atomic curve for $\frac{1}{3}$ Mg $+\frac{2}{3}$ Nb was used. One can see that the limited set of data with $\sin(\theta)/\lambda \leqslant 0.6$ Å^{-1}, such as was used in [6, 10], could be well described both by an undistorted perovskite structure and by the shifts of Pb ions in the high-symmetry direction (anisotropic model) in good agreement with [6, 10]. On the other hand for the complete set of data, large $\sin(\theta)/\lambda$ included, neither the undistorted model, nor the models with ion shifts in any specific high-symmetry direction, give satisfactory agreement with the experimental results. A more or less adequate description was only achieved when the model considered above was used with Pb ions uniformly distributed over the spherical surface. The attempt to apply the same model for the Mg and Nb ions was unsuccessful.

4. Discussion

The physical meaning of these results should be discussed in more detail. The existence of the ion shifts in the high-temperature phase is not very surprising [17]. But it is well known that ions in perovskite-like structures are usually shifted in the high-symmetry directions. However the peculiarity of the PMN crystal is concerned with the fact that non-isovalent ions (Mg^{2+} and Nb^{5+}) are randomly distributed over the equivalent positions. Such random distribution of differently charged ions over the dielectric crystal should result in the appearance of a system of local electric fields random both in values and directions. The consideration that any substitutional defect in a perovskite crystal is symmetry conserving and could not create local fields [18] is not to be applied here because the local surroundings of any ion are not of cubic symmetry and ions are not situated in the centres of symmetry (due to the compositional disorder). The strength of such local fields is of atomic scale and

Model number	T,K	Pb		1/3Mg+2/3Nb		O		E_c	R	χ^2	Commentary
		$\vec{r}$	M	$\vec{r}$	M	$\vec{r}$	M				
1	293K 573K	(0 0 0)	3.554 4.29	(0.5 0.5 0.5)	1.078 1.346	(0.5 0.5 0)	3.252 3.09	3.252 3.375	0.025 0.0194	1.778 0.54	$sin(\theta/\lambda) < 0.6\AA^{-1}$
2	293K 573K	(0 0 0)	5.725 5.15	(0.5 0.5 0.5)	1.18 1.36	(0.5 0.5 0)	2.49 2.43	12.12 5.8	0.136 0.067	4.044 1.54	full set of data
3	293K 573K	(δ 0 0) $\delta = 0.07$ $\delta = 0.063$	2.79 2.81	(0.5 0.5 0.5)	1.05 1.16	(0.5 0.5 0)	2.04 2.28	10.35 4.56	0.114 0.053	3.5 1.34	full set of data
4	293K 573K	(δ δ δ) $\delta = 0.042$ $\delta = 0.039$	2.42 2.6	(0.5 0.5 0.5)	0.98 1.17	(0.5 0.5 0)	2.345 2.42	9.34 4.46	0.11 0.049	3.25 1.22	full set of data
5	293K 573K	(0 0 0)	1.75 2.83	$(0.5+\delta\ 0.5+\delta\ 0.5+\delta)$ $\delta = 0.041$ $\delta = 0.04$	0.24 0.35	(0.5 0.5 0)	5.93 3.75	2.5 0.8	0.25 0.13	6.22 3.48	full set of data fit not converged fit not converged
6	293K 573K	spherical layer radius=Δ $\Delta = 0.285\AA$ $\Delta = 0.259\AA$	1.506 2.34	(0.5 0.5 0.5)	0.84 1.1	(0.5 0.5 0)	1.74 2.51	4.027 3.3	0.0329 0.03	1.03 0.65	full set of data $< u^2 >= 0.14\AA$ $< u^2 >= 0.17\AA$
7	293K 573K	(0 0 0)	5.68 5.13	spherical layer radius=Δ $\Delta = 0.041\AA$ $\Delta = 0.051\AA$	1.1 1.24	(0,5 0.5 0)	2.47 2.406	11.78 6.58	0.136 0.06	4.02 1.54	full set of data

Table 1. E_c, primary extinction parameter [19]; $R = \sum(I_{exp} - I_{calc})/\sum I_{exp}$; χ^2, goodness of fit parameter.

should result in the appearance of large enough random atomic shifts to correspond to the changes of the Madelung energy due to these fields. One could expect that most affected by such atomic scale random fields would be ions situated between non-isovalent ones. Indeed as already described we observe in PMN random shifts of the Pb ions. Neglecting the diffusion processes, the distribution of ions and the resulting system of local fields is 'frozen' and temperature independent. One should also keep in mind that the static shifts are determined by the ion distribution and so their directions could be random, unrelated to the symmetry of the 'average crystal'. As has already been mentioned, after averaging over the crystal volume these shifts would result in a more or less uniform distribution over the spherical layer. The radius of the sphere $\langle\Delta\rangle$ corresponds to the mean value of shift lengths, and the 'thickness' of the layer, defined by the effective Debye–Waller factor, to the dispersion of these lengths $\sigma = \langle\Delta - \langle\Delta\rangle\rangle$. This dispersion has the same order of magnitude as a mean value and increases slightly with increasing temperature.

On the other hand local electric fields should create local dipole moments, interacting with each other. These dipole moments are related mostly to the displacement of so-called ferroelectric active ions, namely—in the case of PMN—the ions in the B-sublattice [22]. The dipole interaction leads to the ordering of these dipole moments in the space scale. Thus in the described system one should expect the appearance of lattice distortions of two kinds—static frozen distortions related to the random distribution of non-isovalent ions and temperature-dependent dynamic distortions, concerned with the local dipole ordering. These temperature-dependent distortions are correlated with the correlation length increase with decreasing temperature [5, 14, 15]. The existence of such correlated displacements is confirmed by the appearance at low temperatures (below 600 K) of strong narrow diffuse scattering with increasing intensity and decreasing width with increasing temperature. At high temperatures, when one could neglect the dipole ordering, experiment shows no diffuse scattering in the vicinities of the reciprocal lattice points, that clearly indicates that static shifts of the lead ions are uncorrelated.

5. Conclusion

Our x-ray measurements have confirmed that even at high temperatures PMN is locally distorted. These distortions are concerned with the shifts of lead ions random both in length and direction. The mean value of shifts length is just slightly temperature dependent and their dispersion is of the same order of magnitude as the mean value. These frozen shifts are probably responsible for the anomalies of the physical properties of PMN at high temperatures.

References

[1] Smolensky G A *et al* 1981 *Ferroelectrics and Related Materials* (New York) p 1
[2] Lines M E and Glass A M 1977 *Principles and Applications of Ferroelectrics and Related Materials* (Oxford)
[3] Kraynik N N, Markova L A, Zhdanova V V, Sapozhnikova L A and Flerova S A 1989 *Ferroelectrics* **90** 119
[4] Dorogovtsev S N and Yushin N K 1990 *Ferroelectrics* **112** 27
[5] Vakhrushev S B *et al* 1989 *Physica* B **156,157** 90
[6] Bonneau P, Garnier P, Husson E and Morell A 1989 *Mater. Res. Bull.* **24** 201
[7] Burns G and Dacol F H 1983 *Solid State Commun.* **48** 853
[8] Siny I G and Smirnova T A 1989 *Ferroelectrics* **90** 191

[9] DeMathan N, Husson E, Calvarin G, Gavarri J R, Hewat A W and Morell A 1991 *J. Phys.: Condens. Matter* **3** 8159
[10] Bonneau P, Garnier P, Calvarin G, Husson E, Calvarri J R, Hewat A W and Morell A 1991 *J. Solid State Chem.* **91** 350
[11] Mylnikova I E and Bokov V A 1961 *Crystal Growth* vol 3 (Moscow: Akademii Nauk USSR) p 438
[12] *SDP Users Guide* 1985 (Delft: Enraf-Nonius) p 376
[13] Aslanov L A *et al* 1989 *Precizionnyi Rentgenosructurnyi Eksperiment* (Moscow: MGU) p 230 (in Russian)
[14] Vakhrushev S B *et al* 1989 *Ferroelectrics* **90** 173
[15] Vakhrushev S B *et al* 1987 *Izv. Akad. Nauk SSSR* **51** 214
[16] Krivoglaz M A 1969 *Theory of X-ray and Thermal-Neutron Scattering by Real Crystals* (New York: Plenum) p 271
[17] Kassan-Ogly F A and Naish V E 1986 *Acta Crystallogr.* B **42** 297
[18] Bruce G and Cowley R A 1981 *Structural Phase Transitions* (London) p 437
[19] Becker P J and Coppens P 1974 *Acta Crystallogr.* A **30** 129
[20] Husson E, Chubb M and Morell A 1988 *Mater. Res. Bul.* **23** 357
[21] Chen J, Chan H M and Harmer M P 1989 *J. Am. Ceram. Soc.* **72** 593
[22] Thomas N J 1990 *J. Phys. Chem. Solids* **51** 1419